Journal of Research and Applications in Mechanical Engineering
ISSN: 2229-2152 (Print); 2697-424x (Online)
(2026) Vol. 14, No. 1, Paper No. JRAME 26-14-009
[DOI: 10.14456/ jrame.2026.9]

*Research Article*

# Experimental insights into heat transfer mechanisms in a turbulent channel flow with inclined V-shaped baffles

**P. Thapmanee**[1]
**C. Homniam**[2]
**A. Phila**[2]
**W. Keaitnukul**[1]
**S. Eiamsa-ard**[2]
**N. Maruyama**[3,4]
**M. Hirota**[5]
**K. Buanak**[6,*]

[1] *Department of Process and Industrial Engineering, School of Engineering and Industrial Technology, Mahanakorn University of Technology, Bangkok, 10530, Thailand.*
[2] *Department of Mechanical Engineering, School of Engineering and Industrial Technology, Mahanakorn University of Technology, Bangkok, 10530, Thailand.*
[3] *Engineering Innovation Unit, Graduate School of Regional Innovation Studies, Mie University, Mie, 514-8507, Japan.*
[4] *Department of Mechanical Engineering, Faculty of Engineering, Mie University, Mie, 514-8507, Japan.*
[5] *Department of Mechanical Engineering, Faculty of Engineering, Aichi Institute of Technology, Aichi, 470-0392, Japan.*
[6] *Department of Automotive-Mechanical Engineering, Faculty of Industrial Technology, Rajabhat Rajanagarindra University, Chachoengsao, 24000, Thailand.*

**Received** 9 October 2024
**Revised** 26 February 2025
**Accepted** 28 February 2025

**Abstract:**
*This study conducts an experimental analysis of heat transfer and pressure drop in a solar air preheater channel with an aspect ratio (AR) of 3.75:1, featuring inclined V-shaped baffles (I-VB) on one wall under continuous heat flux circumstances. The study focuses on the effects of the inclined angles on the heat transfer coefficient (h), pressure drop (ΔP) and thermal-hydraulic performance (THP). The inclined angles (θ) explored include 0°, 45° and 90°, with attack angles (α) set at 45°, and Reynolds numbers (Re) varying from 6000 to 24,000. The experimental results show that the inclined angles significantly affect the temperature distribution, Nusselt number distribution, friction factor, and thermal-hydraulic performance. The heat transfer rates in channels with inclined V-shaped baffles (I-VB) at inclined angles of 0°, 45° and 90° are 13.95-53.46%, 165.29-361.08%, and 175.91-378.34% higher than those in a smooth channel, respectively. However, the corresponding pressure losses increase by 2.01-2.87, 10.42-13.37, and 15.03-19.91 times for these inclined angles. At all Reynolds numbers, the inclined V-shaped baffles with an inclined angle (θ) of 45° demonstrate superior thermal-hydraulic performance, reaching a peak value of 1.94 at a lower Reynolds number of 6000.*

**Keywords:** *Heat transfer coefficient, Inclination angle, V-shaped baffles, Thermal-hydraulic performance*

## 1. Introduction

Solar air heaters are devices designed to capture solar energy and convert it into heat for air heating applications. They typically consist of a flat plate or evacuated tube design, using materials that maximize heat absorption and

* Corresponding author: K. Buanak
E-mail address: kalong@techno.rru.ac.th

minimize heat loss. Efficiency can be enhanced through various strategies, such as optimizing collector geometry, using high-performance absorber materials, integrating thermal storage solutions like phase change materials, and employing advanced control systems. Hybrid systems that integrate solar air heating with photovoltaic technology enhance energy efficiency. Ongoing research focuses on modeling airflow dynamics, experimental validation, and evaluating economic and environmental impacts to ensure sustainability and cost-effectiveness [1]. Techniques for enhancing heat transfer in solar air preheaters are essential for augmenting efficiency and overall performance. These techniques can be categorized as either active or passive methods [2]. Active methods include forced convection systems that use fans or pumps to increase airflow, variable-speed fans for optimized energy use, and the incorporation of nanofluids to boost thermal conductivity. These approaches actively manipulate the heating process, often requiring additional energy input. In contrast, passive methods rely on design features and materials to enhance heat transfer without external energy sources. Techniques such as adding fins, ribs, or baffles to increase surface area, optimizing collector geometry for better airflow, and utilizing high thermal mass materials all contribute to improved efficiency. Combining both active and passive methods can yield significant benefits, leading to more effective solar air heating systems.

Roughening surfaces enhances heat transfer by increasing turbulence and disrupting the boundary layer. Techniques include texturing with laser or chemical etching, using porous materials to increase surface area, and employing 3D printing for complex geometries that promote mixing. These approaches can significantly improve thermal performance in various applications [3]. Numerous studies investigated the impact of baffle geometries—specifically aspect ratio, attack angle, pitch length, and baffle shape—alongside the configuration of baffles (including in-line, staggered, one-wall and opposing two-walls) on Nusselt number, friction factor and thermal-hydraulic performance. Changcharoen and Eiamsa-ard [4] reported a study that examines the impact of detached-rib geometry on the thermal enhancement factor in a rectangular channel. The results indicate that the flow field, temperature distribution, Nusselt number variations, and friction factor are significantly influenced by the ratios of detached clearance. Ribs with a detached-clearance ratio of 0.1 at a Reynolds number of 8000 attain optimal thermo-hydraulic performance. Yongsiri et al. [5] investigated turbulent flow and heat transfer in a channel with inclined detached ribs using the finite volume method. This study compares heat transfer, pressure loss and thermal performance across various attack angles in relation to the standard transversely attached rib. Results indicate that at elevated Reynolds numbers, the ribs oriented at 60° and 120° produce similar heat transfer rates and thermo-hydraulic performance. Luan and Phu [6] employed experimental data to develop correlations for the Nusselt number and friction factor in a solar air collector with inclined baffles. The study evaluates the exergy performance of the collector, indicating maximum errors of 6% for the Nusselt number and 8.3% for the friction factor. The analysis indicates that the maximum collector efficiency attains 0.7% at a baffle angle of 60° and a Reynolds number of 1500. This inclined angle produces the greatest turbulent flow and has a reduced friction factor relative to the angles of 60° and 120°. The thermal efficiency, effective efficiency, and exergy efficiency exhibit nearly identical values, whereas a baffle angle of 0° results in the lowest efficiency observed.

According to the study, only detached or inclined baffles with a small gap ratio have a higher Nusselt number than attached ribs. As the gap ratio increases, the Nusselt number declines because of decreased turbulence intensity in the recirculation zone behind the baffle. Similarly, the gap ratio influences the friction factor, as turbulent intensity, primarily influenced by the size of the recirculation zone, affects both pressure drag and friction. However, the efficiency value of transverse shapes is lower than that of other shape groups. Kumar et al. [7] conducted an experimental study examining the heat transfer characteristics and the optimal relative width parameter of a solar air channel with multiple V-type baffles inclined at 60°. The experiment investigated several parameters, including Reynolds number, relative width, baffle height, pitch, discrete distance, and gap width. The results indicated that a relative baffle width of 5.0 led to improved overall thermal performance, affirming that broken multiple V-type baffles provide enhanced thermo-hydraulic efficiency. Ameur et al. [8] conducted numerical simulations to assess the performance of a channel heat exchanger featuring V-baffles, utilizing a multidimensional CFD model. The research focuses on the effectiveness of vortex generators (baffles) in a complex shear-thinning fluid under laminar flow conditions. The findings indicate that flow rate, baffle orientation and arrangement have a significant impact on heat exchanger efficiency. The study examines two orientations (+V and −V), as well as staggered and aligned arrangements of V-shaped baffles. It turns out that staggered +V baffles have better heat transfer rates.

V-shaped baffles enhance heat transfer by promoting turbulence and fluid mixing, creating complex flow patterns that disrupt boundary layers. While they improve thermal performance, they may also increase pressure drop due to higher resistance, making optimization crucial. Commonly used in heat exchangers and cooling systems, the design

can be tailored by adjusting the angle and spacing of the baffles to suit specific applications. Table 1 presents the conditions investigated in the experimental and numerical studies mentioned above.

**Table 1:** Summarizes the experimental and numerical analyses of notable baffle configurations as documented by many researchers.

| Baffle shapes | Parameter ranges | Major Finding |
|---|---|---|
| Detached-rib [4] 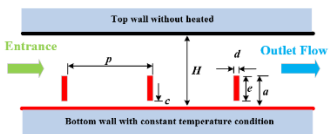  | $c/a$=0.1, 0.2, 0.3 and 0.4<br>$P$=0.5$H$<br>$Re$=8000 to 24,000 | - The SST k-ω turbulence model yields more precise forecasts than the Renormalization Group (RNG) $k$-$\varepsilon$ model.<br>- Detached ribs with a minimal clearance ratio ($c/a$=0.1) produce superior Nusselt numbers, friction factors and thermo-hydraulic performance compared to connected ribs. |
| Inclined detached-ribs [5] 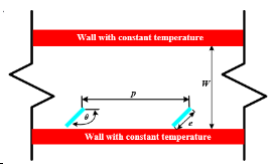  | $\theta$ =0° to 180°<br>$\alpha$=90°<br>$Re$=4000 to 24,000 | - At higher Reynolds numbers (8000≤$Re$≤24,000), angled ribs with attack angles of 45°, 60°, 75°, 105°, 120°, 135° and 150° make recirculation zones that are bigger, but angles of 0°, 15° and 30° and 165° do not. |
| Inclined baffles [6] 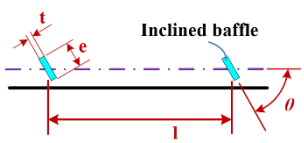  | $\theta$ =0° to 180°<br>$\alpha$=90°<br>$Re$=9000 to 24,000 | - The 60° baffle angle produced the highest efficiencies, whereas a horizontal baffle produced the lowest.<br>- Baffle angles of 30° and 150° produced similar efficiencies, while angles between 60° and 120° were recommended for optimal performance. |
| Broken multiple V-baffle [7] 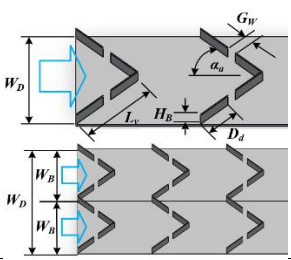 | $W_D/W_B$=1.0 to 6.0<br>$P_B/H_B$=10<br>$\alpha_a$=90°<br>$G_W/H_B$=1.0<br>$Re$=3000 to 8000 | - The augmentation of heat transfer is markedly affected by the ratio of baffle width to base width ($W_D/W_B$), with discontinuous numerous V-type baffles leading to substantial increases in Nusselt number.<br>- In comparison to a solar air channel devoid of baffles, channels featuring broken multiple V-type baffles exhibit elevated values of both Nusselt number and friction factor, which can be ascribed to alterations in fluid flow characteristics that promote reattachment flow, and the formation of jet streams. |
| V-shaped baffles [8] 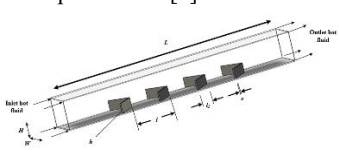 | aligned and staggered arrangement<br>$h/L$=0.033<br>$e/L$=0.008<br>$Re$=0.1 to 300 | - Inserting +V baffles (oriented against the flow) improves fluid interaction and thermal exchange compared to −V baffles, but this results in higher pressure drops.<br>- Staggered baffle arrangements significantly improve heat transfer compared to aligned arrangements. |

Table 1 summarizes experimental studies on important baffle arrangements by a variety of researchers. V-shaped baffles and transverse baffles each offer distinct advantages in heat transfer enhancement. V-shaped baffles generate more turbulence and promote complex flow patterns, leading to improved thermal performance, while transverse baffles are simpler to design and typically result in lower pressure drops. The choice between them depends on factors such as fluid properties, flow rates, and the specific application's thermal requirements. Additionally, inclined baffles and V-shaped baffles typically provide better performance than transverse baffles in thermal applications. However, there has been little research on optimizing the baffles' inclined angle to increase their effectiveness [2, 9].

This study presents an experimental investigation into the performance of a solar air preheater channel incorporating a heated plate with inclined V-baffles as roughness elements. The Reynolds number was varied between 6000 and 24000. The Nusselt number and friction factor were analyzed as functions of roughness parameters, including the inclined angle, to evaluate the thermal efficiency of the system and identify the advantages of this particular roughness geometry.

## 2. Operational Procedure

An experimental method was utilized to collect data on Nusselt number (*Nu*) and friction factor (*f*) for a solar air channel with inclined V-shaped baffle roughness, focusing on the effects of inclined angles on *Nu*, *f* and *THP*.

The experimental investigation encompasses the establishment and configuration of an indoor testing facility. The configuration has been verified by comparing the experimental data acquired without a baffle wall against established standard data. Once validated, extensive experiments were carried out on the inclined V-shaped baffle to collect raw data on heated wall temperatures, air flow rates, inlet and outlet air temperatures, and pressure drop across the channel under stable conditions.

### *2.1 Experimental procedure and experimental setup*

An experimental setup was conceived and constructed to examine the impact of the inclined V-shaped baffle turbulence promoter on Nusselt numbers (*Nu*) and friction factors (*f*) of the air stream. Figure 1 displays a schematic diagram alongside a photographic representation of the arrangement.

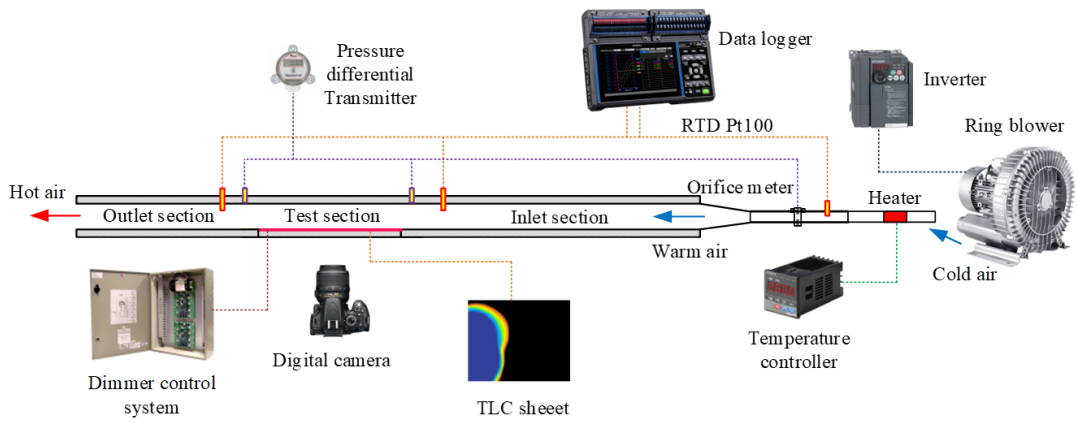


**Fig. 1.** Schematic and photo of the experimental setup with the inclined V-shaped baffle.

The configuration comprised a rectangular acrylic channel linked to a centrifugal blower through a circular PVC pipe. The rectangular channel had a width of 150 mm and a height of 40 mm, resulting in a width-to-height ratio of 3.75. The system comprised inlet and exit sections, which were divided by test sections. The upper wall of the test section consisted of a polyamide sheet heated plate, uniformly heated by an electric heater, ensuring consistent heat flux across the entire bottom wall. The air mass flow rate through the solar air heater was determined using a calibrated orifice meter linked to a pressure differential transmitter sensor. The temperature was assessed at multiple sites utilizing calibrated thermochromic liquid crystal sheets, which were integrated with image processing to visualize the temperature distribution. The wall temperature at various locations was measured using calibrated RTD Pt100 sensors connected to a data acquisition system, which provided input and output temperatures in degrees Celsius with an accuracy of 0.1 °C. Image processing techniques were also employed to visualize the temperature distribution. The air mass flow rate via the duct was quantified using an orifice meter linked to a differential pressure transmitter. The pressure drop across the test section was recorded with a differential pressure transmitter that had a least count of 0.001 in of water. Data were recorded under steady-state conditions, defined as the point at which the plate and air temperatures exhibited negligible variation for approximately 30 minutes. Each test run reached steady state in about 3 hours. To minimize the percentage error in temperature measurements, the minimum heat flux was chosen to raise the air temperature by approximately 10-15 °C. The greatest variation of the non-dimensional parameters was recorded to be 4.8% for the Reynolds number, 4.2% for the Nusselt number, and 3.5% for the friction factor.

### *2.2 Range of parameters*

The dimensions of the solar air heater are as follows: length of 3500 mm, height of 40 mm, and width of 150 mm. The hydraulic diameter, calculated as $D_h=4A_c/P$, is 63.16 mm. The 10 mm thick wall is constructed from acrylic, with

a constant heat flux applied in the range of 250-400 W/m². The baffle parameters are defined by the pitch length ($P$), baffle height ($e$), angle of attack ($\alpha$), and inclined angles ($\theta$). The inclined V-shaped baffle (I-VB) is illustrated in Figure 2 and Table 1 presents the range of these parameters.

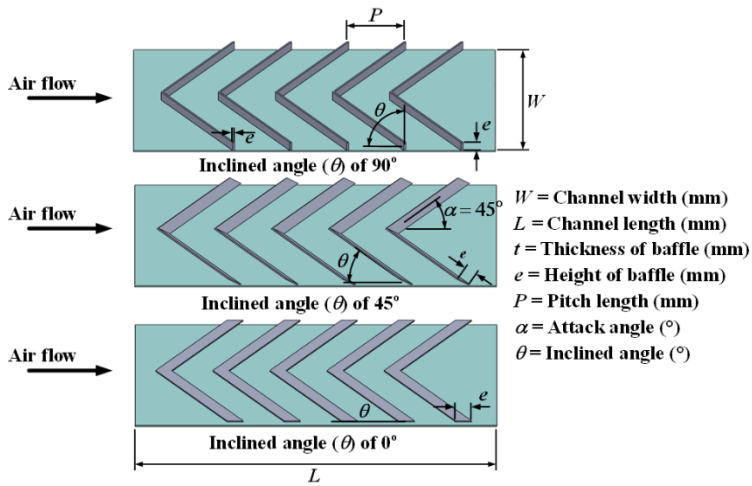


**Fig. 2.** Images of inclined V-shaped baffle at various inclined angles.

**Table 2:** Flow and baffle roughness parameters.

| | |
|---|---|
| *Inclined V-shaped baffle* | |
| Material used for baffling | PLA plastic |
| Thickness of the baffle ($t$) | 1.0 mm |
| Height of the baffle ($e$) | 12.0 mm ($e/H$=0.3) |
| Pitch length ($P$) | 60 mm ($P/H$=1.5) |
| Attack angles ($\alpha$) | 45° |
| Inclined angles ($\theta$) | 0°, 45°, 90° |
| *Solar air heater channel* | |
| Aspect ratio ($AR$) | 3.75 |
| Height of the channel ($H$) | 40 mm |
| Width of the channel ($W$) | 150 mm |
| Length of the channel ($L$) | 900 mm |
| *Working conditions* | |
| Working fluid | Air |
| Reynolds number ($Re$) | 6000-24,000 |
| Prandtl number ($Pr$) | 0.7 |

## 3. Data reduction

The data collected were utilized to compute $Nu$, $f$ and $THP$. Below are the relevant formulas for computing these parameters, along with some intermediate calculations. One important formula is for the weighted average plate air temperature:

### *3.1 Airflow within the solar air heater channel*

The mass flow rate ($m_a$) was determined from the pressure drop data via the calibrated orifice meter utilizing the subsequent formula:

$$m_a = C_d A_o \left[ \frac{2\rho \Delta P}{1-(d_2/d_1)^4} \right]^{1/2} \tag{1}$$

The discharge coefficient ($C_d$) of the orifice meter was determined to be 0.624, following calibration with a hot-wire anemometer. The air velocity ($V$) is determined using the mass flow rate and can be expressed through the following equation:

$$V = \frac{m_a}{\rho A_c} \tag{2}$$

*3.2 Hydraulic diameter*

The hydraulic diameter ($D_h$) is characterized by the subsequent equation:

$$D_h = \frac{4A_c}{P} \tag{3}$$

*3.3 Reynolds number*

The following formula is used to get the Reynolds number assigned to the airflow in the test channel:

$$Re = \frac{VD_h}{\nu} \tag{4}$$

*3.4 Thermo-physical properties of gas*

In order to determine the thermophysical parameters of the gas at atmospheric pressure, the correlations that Duffie and Beckman [10] created were utilized in the calculation process.

$$\rho = 1.204\left(\frac{293}{T}\right) \tag{5}$$

$$\mu = 181\times10^{-5}\left(\frac{T}{293}\right)^{0.735} \tag{6}$$

$$C_p = 1006\left(\frac{T}{293}\right)^{0.0155} \tag{7}$$

$$k = 0.0275\left(\frac{T}{293}\right)^{0.86} \tag{8}$$

*3.5 Temperature measured*

The mean temperature of the plate is determined by averaging all temperatures recorded by the thermochromic liquid crystal sheets (TLCs). The TLC were positioned on the interior bottom wall to track temperature variations on the channel wall surfaces. A high-resolution camera captured changes in the color of the temperature-indicating liquid crystal (TLC), and image processing software assessed the temperature of the channel wall surfaces. The TLC were calibrated using a digital image processing tool under controlled experimental settings, resulting in homogeneous illumination and a constant camera viewing angle [11-12].

*3.6 Coefficient of heat transfer*

The heat transfer coefficient ($h$) for the heated test portion was estimated using the following procedure.

$$h = \frac{Q}{A_w\left(T_w - T_b\right)} \tag{9}$$

The useful heat gained by the air ($Q$) is calculated as follows:

$$Q = m_a C_p\left(T_o - T_i\right) \tag{10}$$

*3.7 Nusselt number*

The Nusselt number ($Nu$) was subsequently calculated utilizing the heat transfer coefficient ($h$), hydraulic diameter ($D_h$), and thermal conductivity ($k$) as illustrated in the equation below:

$$Nu = \frac{hD_h}{k} \tag{11}$$

*3.8 Friction factor*

The friction factor ($f$) was determined using the pressure drop in the test section and the air velocity ($V$) traversing it, applying the fundamental equation defined by Darcy-Weisbach [13].

$$f = \frac{\Delta P}{(L/D_h)\left[\rho\left(V^2/2\right)\right]} \tag{12}$$

*3.9 Thermal efficiency*

The study of the Nusselt number ($Nu$) and friction factor ($f$) indicates that the Nusselt number in the inclined V-shaped baffle channel is significantly enhanced with an increase in the friction factor. It is crucial to choose a geometry that both maximizes the Nusselt number ($Nu$) and minimizes the friction factor ($f$) to the greatest extent possible.

A parameter known as thermo-hydraulic performance (THP) is defined to concurrently evaluate heat transfer and pressure losses. The value of this parameter establishes a relationship between the Nusselt number ($Nu$) and the inclined angles ($\theta$) of the V-shaped baffles per unit pumping power. It compares this relationship to the heat transfer characteristics in a fully developed turbulent flow within the channel, considering both scenarios with and without baffle walls, as detailed in Equation (13) [14-16].

$$THP = \frac{\left(Nu/Nu_s\right)}{\left(f/f_s\right)^{0.33}} \tag{13}$$

**4. Validation of experimental data**

The calculated values of $Nu$ and $f$ from experimental data for a test channel devoid of baffles have been compared with the corresponding data derived from the Dittus-Boelter equation for the Nusselt number, as presented in Equation (14), and the modified Blasius equation for the friction factor, as detailed in Equation (15).

*4.1 Dittus-Boelter equation*

The Dittus-Boelter equation provides the Nusselt number for a smooth channel as follows:

$$Nu_s = 0.023 Re^{0.8} Pr^{0.4} \tag{14}$$

*4.2 Modified Blasius equation*

The friction factor for a smooth channel can be determined using the modified Blasius equation, expressed as follows:

$$f_s = 0.085 Re^{-0.25} \tag{15}$$

## 5. Results and Discussion

An experimental investigation was conducted to investigate the influence of Reynolds number and inclined angles on the Nusselt number and friction factor in a solar air channel equipped with inclined V-shaped baffles that create surface roughness. The results for the channel with inclined V-shaped baffles were compared to those from a smooth surface under similar working conditions, in order to evaluate the enhancements in *Nu* and *f*.

### *5.1 Validation of the experimental apparatus*

Prior to the extensive data collection on rectangular ducts including inclined V-shaped baffles, a validity assessment was conducted. The experimental Nusselt number and friction factor for a smooth channel were ascertained.

Applying the Dittus–Boelter equation, values were computed and compared to the experimental Nusselt number [13–14]. Likewise, the experimentally obtained friction factor values were contrasted with results from the modified Blasius equation [13, 17]. Figure 3 depicts the contrast between the experimental data and the Nusselt numbers and friction factors obtained from the fundamental equations, respectively.

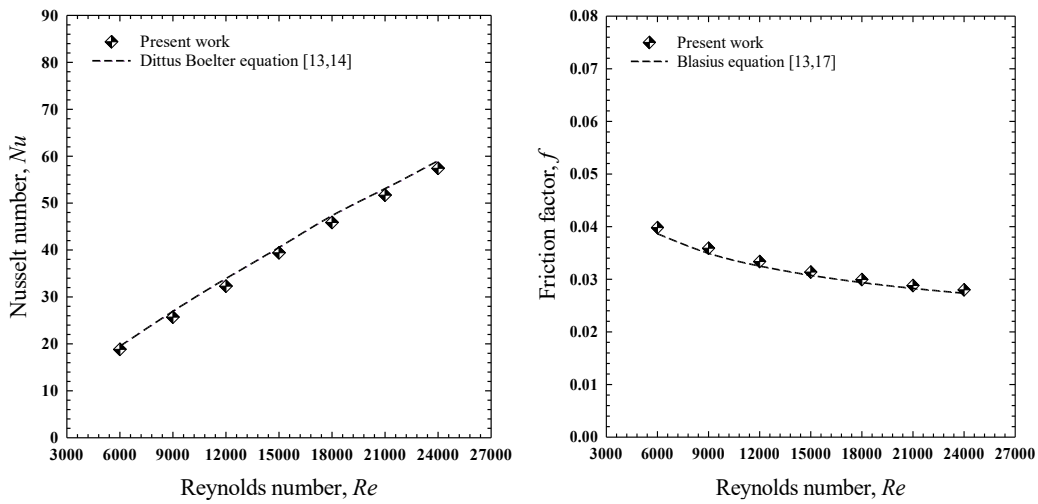


**Fig. 3.** Comparison of experimental and predicted Nusselt number (*Nu*) and friction factor (*f*) data for a smooth channel.

The mean absolute errors between the experimental results and those derived from Equation (13) and Equation (14) were 3.62% for the Nusselt number and 2.47% for the friction factor. These results demonstrate a high degree of accuracy in the experimental measurements.

### *5.2 Heat transfer*

The influence of inclined angles ($\theta$) on the Nusselt number (*Nu*) and friction factor (*f*) in a solar air channel (SAC) is examined. The results were compared with those derived from a smooth surface devoid of baffles under analogous experimental settings.

For the specified parameters, including $e/H$=0.3, $P/H$=1.5, and $\alpha$=45º, the data for the Nusselt number as a function of inclined angle ($\theta$) is presented for various Reynolds numbers (*Re*) in Figure 4.

In comparison to the smooth channel, the configurations featuring inclined V-shaped baffles (I-VB) at different angles ($\theta$=0°, 45° and 90°) demonstrate heat transfer enhancements ranging from approximately 13.95-53.46%, 165.29-361.08%, and 175.91-378.34%, respectively. Notably, the I-VBs with the highest-inclined angle ($\theta$=90°) exhibit the highest efficiency for heat transfer augmentation, producing Nusselt numbers that surpass those at $\theta$=0° and 45° by 142.13-211.71%, and 3.74–5.81%, respectively. In the range studied, angles $\theta$=0°, 45° and 90° resulted in $Nu/Nu_s$ values of approximately 1.14-1.53, 2.65-4.61, and 2.76-4.78 times, respectively, depending on the Reynolds number (*Re*).

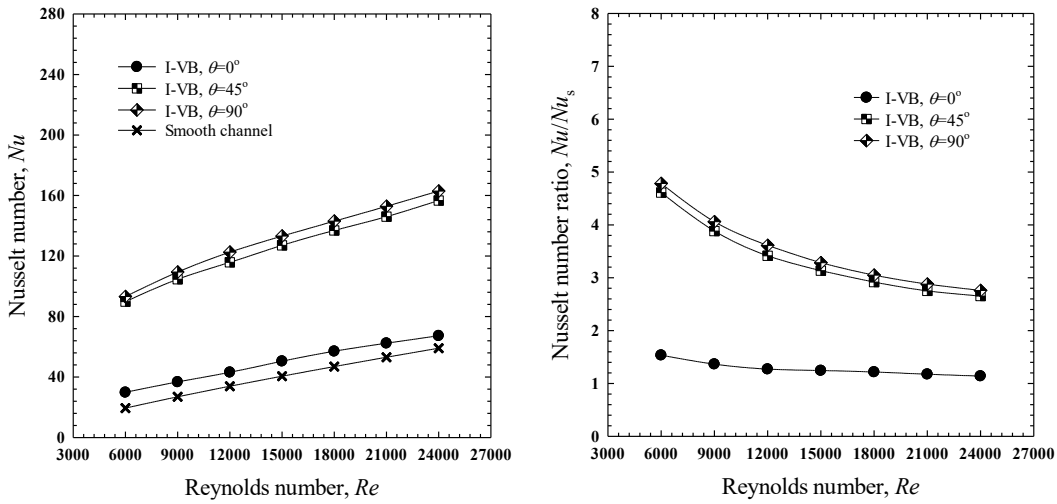


**Fig. 4.** Impact of the inclined angle of V-shaped baffles on the Nusselt number across different Reynolds numbers.

*5.3 Nusselt number and wall temperature field*

Figure (5) and (6) show the Temperature contours and the Nusselt number contours for inclined baffles with inclined angles ($\theta$) varying from 0° to 90°, maintaining $e/H$=0.3, $P/H$=1.5, and $\alpha$=45°, at a Reynolds number of 6000.

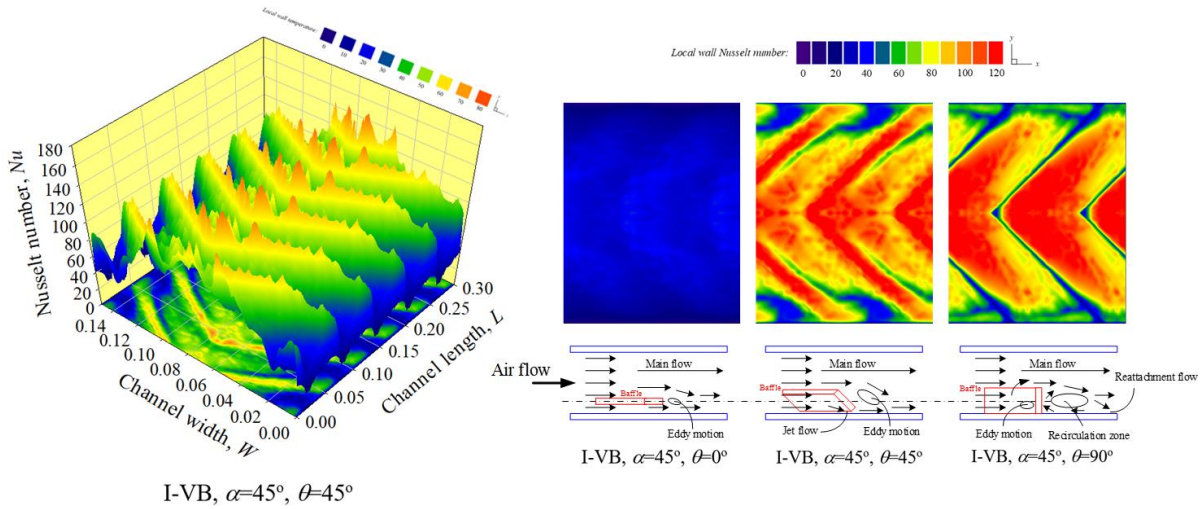


**Fig. 5.** Depiction of local Nusselt number gradients and flow patterns within a test channel.

When $\theta$=0°, the flow characteristics resemble those of a smooth channel. This indicates that the characteristics of the flow under these conditions are consistent with the expected patterns seen in unobstructed channel flow. The influence of the attack angle of inclined V-shaped baffles ($\theta$=45° and 90°) becomes more pronounced with increasing Reynolds numbers, mainly as a result of the generation of recirculation or rotating eddies. This effect increases fluid mixing between the core and tube surface regions due to turbulent fluctuations and baffle element eddy motion. It can be observed that raising the inclined angle ($\theta$) from 0° decreases the gap height between the baffle and the channel wall, resulting in the generation of secondary stream flow that enhances the Nusselt numbers ($Nu$), as depicted in Figure (5). However, the Nusselt number continues to increase only up to an angle of 90°. Inclined V-shaped baffles ($\theta$=45°) generate powerful secondary stream jets in the gap beneath the baffle along the surface wall, promoting turbulent mixing as these jets reattach and merge with the main flow. As illustrated in Figure (5) and (6), the temperature distribution will influence the Nusselt number distribution in an opposing manner. Areas with elevated heat transfer will show an increase in the Nusselt number alongside a reduction in temperature.

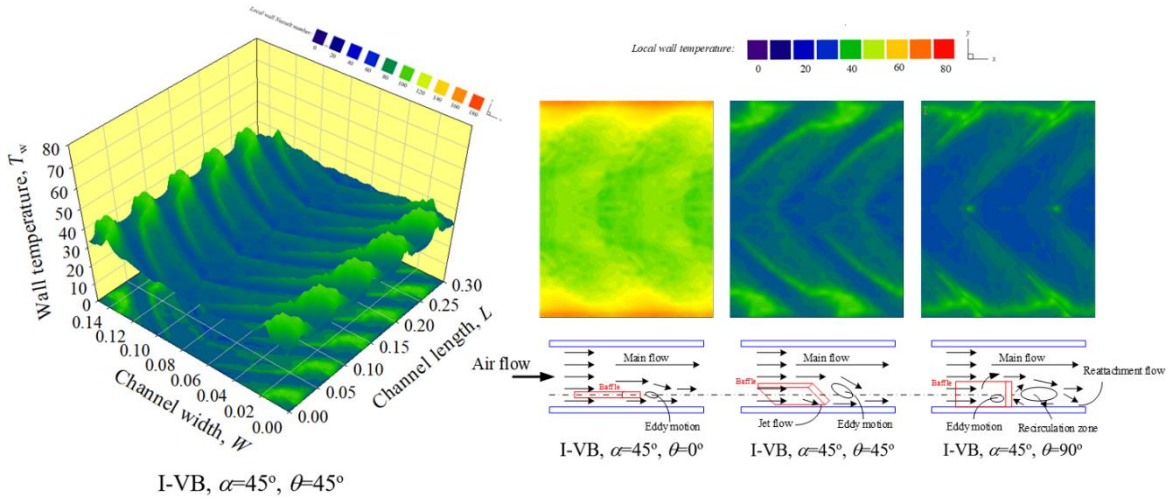


**Fig. 6.** Depiction of local wall temperature gradients and flow patterns within a test channel.

*5.4 Friction factor*

Plots of friction factor ratio ($f/f_s$) versus Reynold number ($Re$) at various inclined angles ($\theta$) are presented in Figure (7). In all scenarios, an increase in the Reynolds number ($Re$) resulted in higher ($f/f_s$) ratios, attributed to increased turbulence and wall shear stress, which in turn led to greater flow resistance. Across the examined range, inclined V-shaped baffles demonstrated friction losses that were 2.01 to19.91 times higher than those observed in a smooth channel for Re values between 6,000 and 24,000.

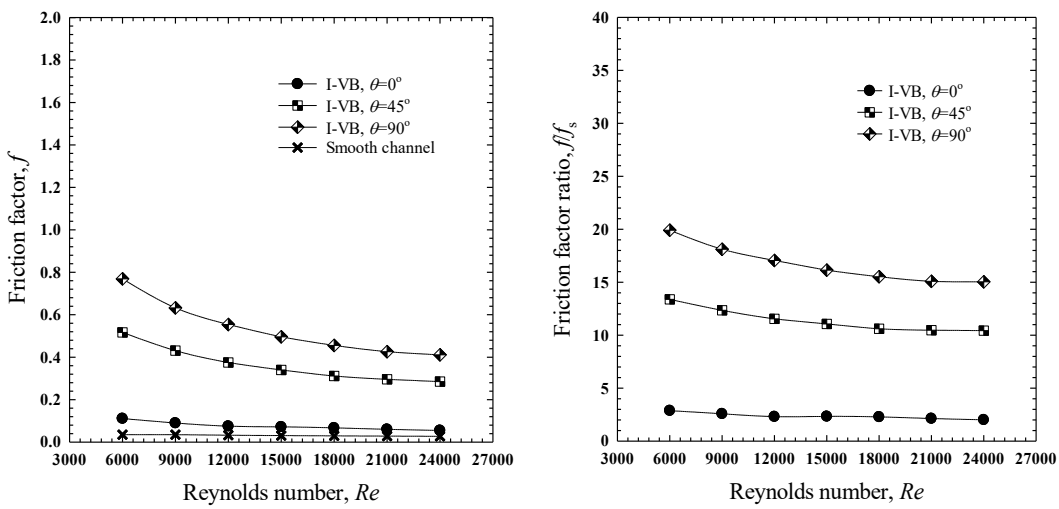


**Fig. 7.** Impact of the inclined angle of V-shaped baffles on the friction factor across different Reynolds numbers.

At a given $Re$, higher $\theta$ values corresponded to increased flow obstruction, turbulence, and wall shear stress, which contributed to greater flow resistance and subsequently higher friction factor ratio ($f/f_s$) values. Conversely, a decrease in $\theta$ had the opposite effect, as reduced flow obstruction resulted in lower turbulence and wall shear stress, leading to decreased flow resistance. Across the studied range, inclined V-shaped baffles at $\theta$=0°, 45° and 90° yielded friction factor ratios ($f/f_s$) of 2.01-2.87, 10.43-13.38, and 15.04-19.91 times, respectively, depending on $Re$, and $\theta$ values. Notably, $\theta$=90° resulted in friction factor ratio ($f/f_s$) values that were 578.95-647.94% and 44.06-48.82% higher than those at 0° and 45°, respectively. The maximum friction factor ratio ($f/f_s$) value reached approximately 19.91 with the inclined V-shaped baffles at $\theta$=90°, $e/H$=0.3, $P/H$=1.5, $\alpha$=45°, and $Re$=24,000.

*5.5 Thermo-hydraulic performance*

Figure 8 illustrates the effect of the inclined angle of V-shaped baffles on thermo-hydraulic performance across different Reynolds numbers. At low Reynolds numbers (*Re*=6000 and 9000), the thermo-hydraulic performances for all configurations are comparable and exceed one. In contrast, at higher Reynolds numbers (*Re*=12,000 and 24,000), the influence of the inclined attack angle becomes pronounced. Significantly, the inclined ribs at angles of $\theta$=45° and 90° demonstrate similar thermo-hydraulic performances (greater than one) throughout the entire range analyzed. In contrast, baffles with smaller inclined angles ($\theta$=0°) yield thermal performance factors below one. These findings indicate that energy savings can be realized by utilizing inclined detached ribs with angles of 45° and 90°.

At inclined angles ($\theta$) of 0°, 45° and 90°, the thermo-hydraulic performance (*THP*) values varied from approximately 0.91 to 1.28, 1.21 to 1.94, and 1.12 to 1.76, respectively, depending on the Reynolds number (*Re*) and the inclined angle ($\theta$). Notably, a $\theta$ of 45° resulted in *THP* values that were 5.26%, and 26.79% higher than those for $\theta$ values of 0° and 90°, respectively. The peak *THP* of 1.94 was recorded at $\theta$=45°, *e*/*H*=0.3, *P*/*H*=1.5, and $\alpha$= 45° under the lowest Reynolds number conditions.

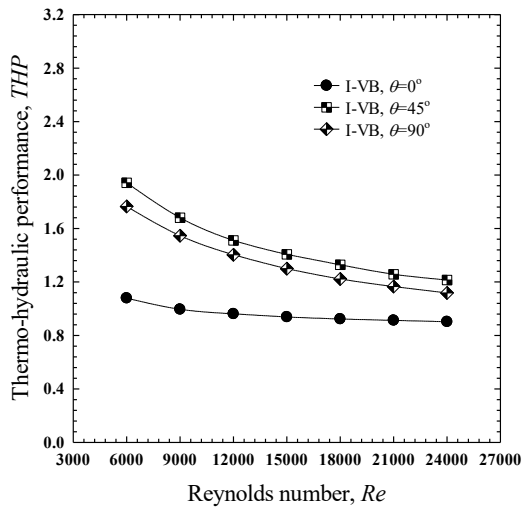


**Fig. 8.** Impact of the inclined angle of V-shaped baffles on the thermo-hydraulic performance across different Reynolds numbers.

## 6. Empirical correlations

The thermal performance for determining optimal parameters for inclined V-shaped baffles can be accurately predicted using relevant correlations. Least-squares regression provides an effective approach for data correlation. This study revealed that the Nusselt number (*Nu*) was influenced by the Reynolds number (*Re*), Prandtl number (*Pr*), and inclined angle ($\theta$), but the friction factor (*f*) was determined to be independent of the Prandtl number (*Pr*). The empirical correlations are outlined in Equations (16) to (17):

$$Nu = 0.3836 Re^{0.4639} Pr^{0.4} \left(15+\theta\right)^{0.3565} \tag{16}$$

$$f = 2.0461 Re^{-0.4615} \left(15+\theta\right)^{0.6701} \tag{17}$$

Figure 9 compares the experimental correlations for the Nusselt number (*Nu*) and the friction factor (*f*) with the values predicted by Equations (16) and (17). The predicted values for *Nu* and *f* differ from the experimental measurements by approximately 2.42% to 8.12%.

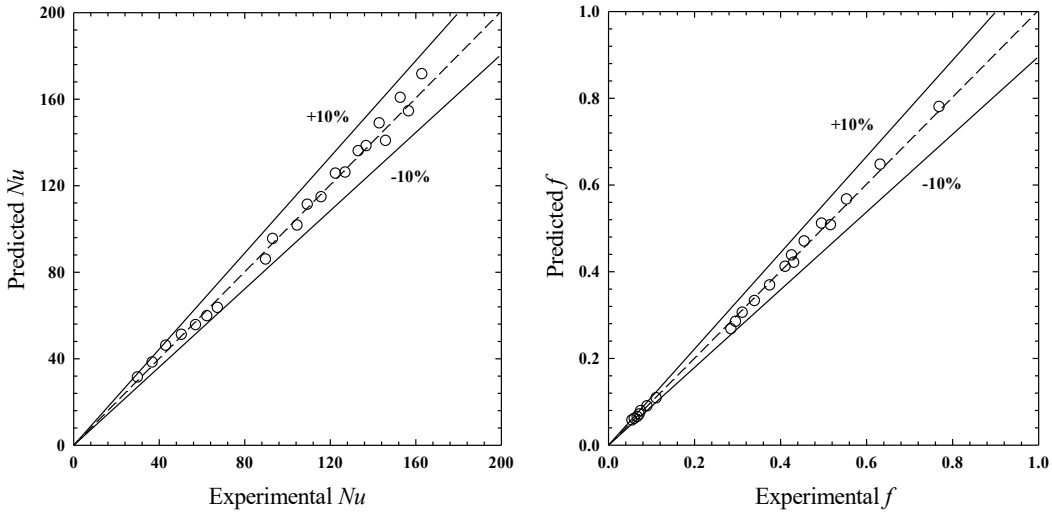


**Fig. 9.** The correlation between expected and experimental values for the Nusselt number (*Nu*) and friction factor (*f*) for inclined V-shaped baffles.

## 7. Comparison with related works

Figure 10 shows a comparison of the thermo-hydraulic performance (*THP*) of inclined V-shaped baffles (I-VB) at angles of $\theta$=45° (mid-angle) and 90° (maximum angle) against results from other investigations on alternative baffle configurations. These encompass detached rib [4], inclined detached-ribs [5], inclined baffle [6], sine wave baffles [18], broken multiple V-type baffle [7], alternate axis twisted baffles [11], notched baffles [19], delta-wing perforated V-type baffles [20], as well as W-shaped rib [21].

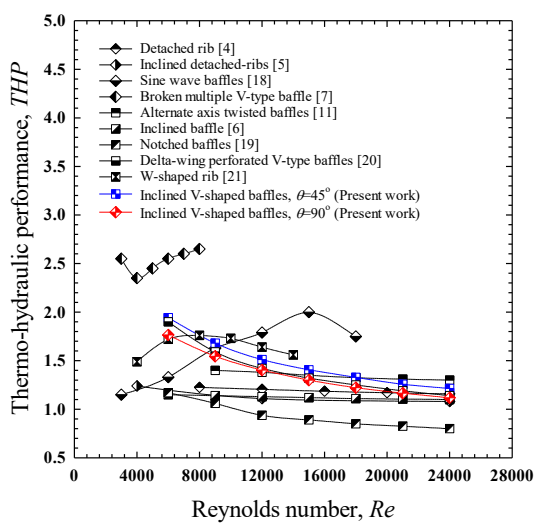


**Fig. 10.** Compares the thermo-hydraulic performance (*THP*) from earlier research.

The benchmarking indicates that the I-VB ($\theta$=45° and 90°) demonstrate the highest thermo-hydraulic performance (*THP*) values. The thermo-hydraulic performance (*THP*) of the inclined V-shaped baffle (I-VB) is comparable to that of the sine wave baffles [18], delta-wing perforated V-type baffles [20], W-shaped rib [21], alternate axis twisted baffles [11], higher than that of the detached rib [4], inclined detached-ribs [5], inclined baffle [6] as well as the notched baffles [19], but lower than the thermo-hydraulic performance (*THP*) of the broken multiple V-type baffle [7].

## 8. Conclusions

The impact of inclined V-shaped baffles at different inclined angles ($\theta$=0°, 45° and 90°) on heat transfer, friction factor, and thermo-hydraulic performance has been studied experimentally for Reynolds numbers between 6,000 and 24,000. The experimental findings reveal that:

(1) At elevated Reynolds numbers ($Re$=6,000 to 24,000), inclined V-shaped baffles with inclined angles ($\theta$) of 45° and 90° create larger recirculation zones, whereas inclined V-shaped baffle with smaller inclined angles ($\theta$=0°) do not.

(2) The inclined V-shaped baffles that promote recirculation demonstrate elevated Nusselt numbers and friction factors compared to those that do not.

(3) The inclined V-shaped baffles demonstrate superior Nusselt numbers ($Nu$) and friction factors ($f$) when compared to a solar air channel that is missing baffles. Changes in fluid flow characteristics occur as a result of the baffle roughness, leading to phenomena such as flow separation, reattachment, and the generation of secondary flow jets.

(4) Among the tested inclined V-shaped baffles, those with $\theta$=90° achieve a heat transfer rate that is 2.76-4.78 times greater than that of the smooth channel, outperforming the other configurations.

(5) The inclined V-shaped baffles that facilitate recirculation exhibit higher Nusselt numbers and friction factors than their counterparts.


## Acknowledgments

This research was financially supported and facilitated by the School of Engineering and Industrial Technology at Mahanakorn University of Technology.


## Nomenclature

| | |
|---|---|
| $AR$ | aspect ratio |
| $A_c$ | cross section area, $m^2$ |
| $A_w$ | heat transfer surface area, $m^2$ |
| $a$ | total height of clearance and rib, m |
| $C_d$ | discharge coefficient for the orifice meter |
| $C_p$ | specific heat of fluid, J/kg-K |
| $D_h$ | hydraulic diameter, m |
| $d_1$ | diameter of orifice, m |
| $d_2$ | diameter of orifice tube, m |
| $c$ | height of clearance, m |
| $e$ | thickness of rib, m |
| $e$ | baffle height, m |
| $f$ | friction factor |
| $f_s$ | friction factor for a smooth channel |
| $G$ | gap width, m |
| $H$ | channel height, m |
| $h$ | rib height, m |
| $h$ | convective heat transfer coefficient, $W/m^2$-K |
| I-VB | inclined V-shaped baffle |
| $k$ | thermal conductivity of fluid, W/m-K |
| $L$ | length of test section, m |
| $m_a$ | mass flow rate, kg/s |
| $Nu$ | Nusselt number |
| $Nu_s$ | Nusselt number for a smooth channel |
| $P$ | pitch length, m |
| PVC | Polyvinyl Chloride |
| $Pr$ | Prandtl number |
| $\Delta P$ | pressure drop, Pa |
| $Q$ | heat gained of air, W |
| $Re$ | Reynolds number |

| | |
|---|---|
| $T_b$ | bulk air temperature, K |
| $T_i$ | inlet air temperature, K |
| $T_o$ | outlet air temperature, K |
| SAC | solar air channel |
| THP | thermal-hydraulic performance |
| TLC | thermochromic liquid crystal |
| $t$ | thickness of baffle, m |
| $V$ | air velocity, m/s |
| $W$ | baffle width, m |
| $W$ | channel width, m |
| $\alpha$ | attack angle, degree |
| $\theta$ | inclined angle, degree |
| $\rho$ | fluid density, kg/m$^3$ |
| $v$ | kinematic viscosity, m$^2$/s |

**References**


[1] Sharma SK, Kalamkar VR. Thermo-hydraulic performance analysis of solar air heaters having artificial roughness: A review. Renewable and Sustainable Energy Reviews. 2015;41:413–435.

[2] Bao S, Deng H, Zhang Z, Hu R, Liu G. Heat transfer enhancement method for high-voltage cable joints in tunnels. International Journal of Thermal Sciences. 2023;183:107872.

[3] He Y, Tang SZ, Tao WQ, Li MJ, Wang FL. A general and rapid method for performance evaluation of enhanced heat transfer techniques. International Journal of Heat and Mass Transfer. 2019;145:118780.

[4] Changcharoen W, Eiamsa-ard S. Numerical investigation of turbulent heat transfer in channels with detached rib-arrays. Heat Transfer – Asian Research. 2011;40(5):431–447.

[5] Yongsiri K, Eiamsa-ard P, Wongcharee K, Eiamsa-ard S. Augmented heat transfer in a turbulent channel flow with inclined detached-ribs. Case Studies in Thermal Engineering. 2014;3:1–10.

[6] Luan NT, Phu NM. Thermohydraulic correlations and exergy analysis of a solar air heater duct with inclined baffles. Case Studies in Thermal Engineering. 2020;21:100672.

[7] Kumar R, Kumar A, Chauhan R, Sethi M. Heat transfer enhancement in solar air channel with broken multiple V-type baffle. Case Studies in Thermal Engineering. 2016;8:187–197.

[8] Ameur H, Sahel D, Menni Y. Enhancement of the cooling of shear-thinning fluids in channel heat exchangers by using the V-baffling technique. Thermal Science and Engineering Progress. 2020;18:100534.

[9] Momin AE, Saini JS, Solanki SC. Heat transfer and friction in solar air heater duct with V-shaped rib roughness on absorber plate. International Journal of Heat and Mass Transfer. 2002;45:3383–3396.

[10] Duffie JA, Beckman JA. Solar Engineering of Thermal Processes. New York: Wiley Inter Science Publications; 1980.

[11] Phila A, Thianpong C, Eiamsa-ard S. Influence of geometric parameters of alternate axis twisted baffles on the local heat transfer distribution and pressure drop in a rectangular channel using a transient liquid crystal technique. Energies. 2019;12:2341.

[12] Narato P, Wae-hayee M, Abdullah MZ, Nuntadusit C. Effect of inclined pins on flow and heat transfer characteristics for single row in rectangular channel. Journal of Research and Applications in Mechanical Engineering. 2017;5(2):106–118.

[13] Alam T, Saini RP, Saini JS. Experimental investigation on heat transfer enhancement due to V-shaped perforated blocks in a rectangular duct of solar air heater. Energy Conversion and Management. 2014;81:374–383.

[14] Promvonge P, Phila A, Chuwattanakul V, Chokphoemphun S, Eiamsa-ard S, Maruyama N, Hirota M. Effect of arc-shaped twisted-baffles on augmented heat transfer in a rectangular duct. Case Studies in Thermal Engineering. 2023;42:102754.

[15] Promthaisong P, Boonloi A, Jedsadaratanachai W. Numerical analysis of turbulent heat transfer in a square channel with V-baffle turbulators. Journal of Research and Applications in Mechanical Engineering. 2014;2(2):122–130.

[16] Hoonpong P, Skullong S. Performance improvement of solar air heater with V-baffles on absorber plate. Journal of Research and Applications in Mechanical Engineering. 2014;6(1):29–39.

[17] Aharwal KR, Gandhi BK. Experimental investigation on heat-transfer enhancement due to a gap in an inclined continuous rib arrangement in a rectangular duct of solar air heater. Renewable Energy. 2008;33:585–596.

[18] Sharma S, Das RK, Kulkarni K. Computational and experimental assessment of solar air heater roughened with six different baffles. Case Studies in Thermal Engineering. 2021;27:101350.
[19] Phila A, Keaitnukul W, Eiamsa-ard S, Naphon P, Maruyama N, Hirota M, Chuwattanakul V. Influence of notched baffles on aerothermal performance behaviors in a channel. Case Studies in Thermal Engineering. 2023;47:103070.
[20] Eiamsa-ard S, Phila A, Thianpong C, Chuwattanakul V, Maruyama N, Hirota M. Enhanced heat transfer performance in channel with delta-wing perforated V-type baffles. Journal of Thermal Analysis and Calorimetry. 2023;148:11283–11301.
[21] Lanjewar A, Bhagoria JL, Sarviya RM. Heat transfer and friction in solar air heater duct with W-shaped rib roughness on absorber plate. Energy. 2023;36:4531–4541.